Desert dust, industrialization and agricultural fires: Health impacts of outdoor air pollution in Africa

Susanne E. Bauer [1], Ulas Im [2], Keren Mezuman [3,1], Chloe Y. Gao [3,1]

NASA Goddard Institute for Space Studies, New York, NY, USA (1)
Aarhus University, Department of Environmental Science, Roskilde, Denmark (2)
Department of Earth and Environmental Sciences, Columbia University, New York, NY, USA (3)

Abstract

The African continent continuously experiences extreme aerosol load conditions, during which the World Health Organizational (WHO) clean air standard of 10 μgm^{-3} of $PM_{2.5}$ mass is systematically exceeded. Africa holds the world largest source of desert dust emissions, undergoes strong industrial growth, and produces approximately a third of the Earth's biomass burning aerosol particles. Sub-Saharan biomass burning is driven by agricultural practices, such as burning fields and bushes in the post-harvest season for fertilization, land management and pest control. Thus, these emissions are predominantly anthropogenic. Here we use global atmospheric composition, climate, and health models to simulate the chemical composition of the atmosphere and calculate the mortality rates for Africa by distinguishing between purely natural, industrial/domestic and biomass burning emissions. Air quality related deaths in Africa rank within the top leading causes of death in Africa. Our results of ~780,000 premature deaths annually point to the extensive health impacts of natural emissions, high mortality rate caused by industrialization in Nigeria and South Africa, and to a smaller extent by fire emissions in Central and West Africa. 43,000 premature deaths in Africa are linked to biomass burning mainly driven by agriculture. Our results also show that natural sources, in particular windblown dust emissions, have large impacts on air quality and human health in Africa.

1. Introduction

Our understanding of the impacts of outdoor air pollution on health in African is limited (Petkova et al., 2013). Obstacles in carrying out this research, in addition to political and societal reasons, are caused by the lack of epidemiological studies (Ahmed et al., 2017) and observational datasets monitoring atmospheric composition. Air quality monitoring networks currently only exist in South Africa and are in the planning for Ghana (Amegah and Agyei-Mensah, 2017). Air quality networks, particularly in Sub-Saharan Africa, have been stalled or discontinued in recent years (Petkova et al., 2013). A small number of field campaigns has helped to study atmospheric composition in Africa. The African Monsoon Multidisciplinary Analysis (AMMA) campaign in West Africa performed atmospheric composition measurements during the Monsoon season in 2006 (Reeves et al., 2010) and supports continuous measurement stations in the Sahel, the Sahelian Dust Transect (Marticorena et al., 2010). Further field campaigns include the Southern African Regional Science Initiative SAFARI (Swap et al., 2002) performed during the dry season in 2000, and currently, the

Dynamics–Aerosol– Chemistry–Cloud Interactions in West Africa (DACCIWA) campaign (Knippertz et al., 2017) is studying aerosol cloud interactions in West Africa, as well as, the ObseRvations of Aerosols above CLouds and their intEractionS (ORACLES) (Zuidema et al., 2016), the Cloud-Aerosol-Radiation Interactions and Forcing (CLARIFY) and the Aerosol Radiation and Clouds in Southern Africa (AEROCLO-Sa) campaigns studying aerosol clouds interactions in the marine stratocumulus deck off the coast of Africa over the South East Atlantic.

In addition, important work has been carried out to improve African emission inventories (Assamoi and Liousse, 2010; Liousse et al., 2014; Marais and Wiedinmyer, 2016). However, other than the mentioned exceptions, long-term surface observational networks are almost non-existent on the entire continent, leaving observations from space and modeling as the only alternative to studying air pollution in Africa.

Only few studies exist outside of urban areas addressing health and air quality in Africa. This stands in great contrast to the severity of the problem itself. African countries, such as Nigeria and Egypt (Lelieveld et al., 2015), are among the leading countries of deadly air pollution. With some of the world's largest sources of pollutants, fastest population growth, and most persistent poverty, Africa is a unique region and its air pollution presents a pressing problem. Air pollution emitted in Africa comes from natural sources, anthropogenic sources, and a mix of natural and anthropogenic aerosols released by biomass burning. There is a fine interplay between these sources. For example, anthropogenic emissions can change dust storm locations and frequency through climate feedbacks as we will show here in this study. Thus, anthropogenic activity can also impact natural emissions. African biomass burning activities, generally categorized as savanna, forest and agricultural waste burning, are driven by the 'slash and burn' agricultural practices that take place during the dry season, which is late October to early March in the Northern Hemisphere and early May to early October in the Southern Hemisphere (Giglio et al., 2013; Magi et al., 2012). In addition, Central Africa experiences the largest lightning flash rates globally (Cecil et al., 2014; Christian et al., 2003), which affects air pollution through natural fire emissions (Goldammer and Price, 1998), and generation of tropospheric nitric oxides NOx's (Murray, 2016; Schumann and Huntrieser, 2007). Biomass burning can also lead to significant increase in the air pollutant surface ozone. In fact, (Aghedo et al., 2007) found that surface ozone rises by 50 ppbv during the burning season in Central Africa.

This complex atmospheric composition scheme is further complicated by a fast-growing society. Africa currently has the fastest growing population in the world, which is projected to more than double between 2010 and 2050, surpassing two billion (UN 2011). By 2050, nearly 60% of the African population is predicted to be living in cities, compared to less than 40% in 2011 (UN 2012) (Amegah and Agyei-Mensah, 2017). The urban population in Africa is anticipated to increase by a factor of 3 over the next 40 years (UN 2012, (Lacey et al., 2017)). Such trends will further increase future mortality due to climate change (Silva et al., 2017) predicted for the African continent.

Societal factors such as poverty and development also need to be considered when discussing health in Africa. Urbanization is a powerful driver of the global demographic and epidemiologic transition, characterized by declining birth rates, increased life expectancy, and a shift from

traditional threats, such as infectious diseases and malnutrition, to chronic and noncommunicable diseases, such as heart disease and diabetes (Petkova et al., 2013).

Previous modeling studies found that exposure to outdoor air pollution has led to 176,000 deaths and 626,000 Disability-Adjusted Life Years in Sub-Saharan Africa (Amegah and Agyei-Mensah, 2017) and it is expected that these numbers are much higher in reality due to the limited data emanating from the region. (Lacey et al., 2017) used an updated emission inventory by (Marais and Wiedinmyer, 2016) and estimated 13,210 annual premature deaths in Africa from all anthropogenic sectors across the continent for present day, without including the impact of biomass burning. (Evans et al., 2013) estimated the expected number of deaths from all causes, cardiopulmonary diseases, lung cancer, and ischemic heart disease, due to chronic $PM_{2.5}$ exposure. They used risk coefficients based on the acute coronary syndrome (ACS) cohort study and $PM_{2.5}$ concentrations from satellite retrievals. In their assessment, they separated the impact of all air pollution and that of dust aerosol on mortality. They found that the $PM_{2.5}$ mortality in the Mediterranean region (several countries in North Africa and the Middle East) was mainly related to the non-anthropogenic component of total $PM_{2.5}$. In their base case scenario, they estimated approximately 2.48 million deaths globally for cardiopulmonary disease (CPD) and 222,000 for lung cancer attributed to total $PM_{2.5}$ in 2004, and after the removal of the natural dust component, they found approximately 1.65 million and 170,000 CPD and lung cancer deaths, respectively. The difference in mortality of about 830,000 for CPD and 52,000 for lung cancer indicates the impact of natural dust.

Data compiled by the Global Burden of Disease (GBD) (Wang et al., 2017) found that since 2000, the percentage of deaths (from lower respiratory infections, ischemic heart disease, and stroke) in Africa impacted by ambient concentrations $PM_{2.5}$ has risen from 16.8 percent of the total global deaths to 19.3 percent in 2012 (Forouzanfar et al., 2015). Recent estimates of 188,000 annual premature deaths are due to ambient $PM_{2.5}$ air pollution from both natural and anthropogenic sources in Africa, with approximately 38 percent occurring in Nigeria (Lelieveld et al., 2015). (Heft-Neal et al., 2018) estimates that $PM_{2.5}$ concentrations above minimum exposure levels were responsible for 22% of infant deaths in 30 studied countries in Africa and led to 449,000 infants death in 2015.

This brief overview reveals that mortality numbers vary significantly, underlining the large uncertainty in air pollution health studies in general, and particularly for Africa. Here we want to apply a different approach. In this study, we will use a global climate model that includes sophisticated aerosol microphysics (Bauer et al., 2008) in combination with the Economic Valuation of Air Pollution (EVA) system (Brandt et al., 2013a; 2013b; Im et al., 2018) to calculate premature mortality in Africa under consideration of $PM_{2.5}$ and gaseous pollutants such as ozone, carbon monoxide (CO), and sulfur dioxide (SO_2). This study differs from previous health studies by specifically quantifying air pollution from natural and anthropogenic sources for the African continent and considering internally mixed aerosol particles. Further this study allows feedbacks between atmospheric composition and interactive natural emissions to take place. Model evaluation are performed mostly with satellite observations and some available surface

measurements, and source - receptor analysis is included to isolate anthropogenic and natural pollutant sources, with a special emphasis on biomass burning emissions.

2. Method

2.1 GISS climate model:

This study is based upon the NASA GISS climate model, GISS-E2.1, an updated version form model GISS-E2 (Miller et al., 2014; Schmidt et al., 2014). Updates include improvements to convection and representation of the Madden-Julian Oscillation MJO (Kim et al., 2012), updates and corrections to the radiative transfer code, ocean mixing, sea ice thermodynamics among other changes, while maintaining the same overall vertical and horizontal resolution, 2° by 2.5° horizontally and 40 vertical layers, with the model top at 0.1 hPa. The model is coupled to the aerosol microphysical scheme, Multiconfiguration Aerosol TRacker of mIXing state (MATRIX) (Bauer et al., 2008). MATRIX resolves aerosol microphysical processes such as new particle formation, condensation and coagulation, leading to evolving size distributions and internally mixed aerosol species (Bauer et al., 2013). Carrying only two moments requires additional information about the shape of the individual aerosol size distributions. We assume a lognormal distribution with constant width when calculating the initial size distributions, the conversion between aerosol mass and number concentration, emission distributions, coagulation rates, and aerosol optical properties. For each aerosol population, defined by mixing state, the tracked variables are number concentration and mass concentration of sulfate, nitrate, ammonium, aerosol water, black carbon, organic carbon, mineral dust, and sea salt. The model simulated a full decade, from 2007 to 2017, nudged to NCEP horizontal winds. Sea salt and dust emission fluxes are calculated interactively. Additional natural and anthropogenic fluxes are from the CMIP6 inventory (Hoesly et al., 2018; van Marle et al., 2017). Supplementary to the base runs, three experiments were performed: one with no anthropogenic emissions, another with no biomass burning emissions, and lastly, one considering natural sources except biomass burning. These experiments were used to calculate the 'natural', the 'industrial/domestic', and the 'biomass burning' effects of the individual emission sectors on surface concentrations of gases and aerosols. All results presented here, unless otherwise marked, including the health analysis are for the year 2016.

2.2 Health Analysis: EVA model description

The EVA system (Brandt et al., 2013a) is based on the impact-pathway chain method (e.g. (Friedrich and Bickel, 2001)), and it calculates health impacts of air pollution due to exposure to outdoor air pollution levels and the associated external costs. The EVA system requires hourly gridded concentrations along with gridded population data, exposure-response functions (ERFs) for health impacts, and economic valuations functions of the impacts from air pollution. A detailed description of the integrated EVA model system along with the ERFs and the economic valuations used are provided by (Brandt et al., 2013a; 2013b; Im et al., 2018). The EVA system can estimate various health impacts, including different morbidity outcomes as well as short-term (acute) and long-term (chronic) mortality, related to short term (acute) exposure to O_3, CO, and SO_2, and long

term (chronic) exposure to $PM_{2.5}$. EVA calculates and uses the annual mean concentrations of CO, SO_2, and $PM_{2.5}$, while for O_3, it uses the SOMO35 metric that is defined as the annual sum of the daily maximum of 8-hour running average over 35 ppb, following WHO (2013) and EEA (2017). In addition, EVA uses population densities over fixed age intervals, corresponding to babies, children, adults and the elderly (Table 1). Age fractions for the African region were extracted from the United Nations (https://esa.un.org/unpd/wpp/Download/Standard/Population/) for the year 2016.

Table 1. Age fractions for the African continent used in the EVA system.

Age Categories	Africa (%)
<1	3.88
<=15	43.48
>=16	56.53
>30	31.80
>65	3.50

ERF for all-cause chronic mortality due to $PM_{2.5}$ were based on the findings of (Pope et al., 2002), which are then extensively used and supported by the scientific review of the Clean Air For Europe (CAFÉ) program and more recently by the latest HRAPIE project report (WHO, 2013a). In the present study, we have used a cutoff value of 8.8 μgm^{-3} for annual mean $PM_{2.5}$, following previous studies (WHO, 2013a,b). Regarding O_3, EVA uses ERFs from the CAFÉ for post-natal death (age group 1–12 months) and acute death related to O_3 (Hurley et al., 2005). There are also studies showing that SO_2 is associated with acute mortality, and EVA adopts the ERF identified in the APHENA study – Air Pollution and Health: A European Approach (Katsouyanni et al., 1997).

3. Evaluation

Because of the specific interest in African air pollution, the model performance is analyzed over the African continent. Unfortunately, this part of the world is poorly observed and lacks reliable observational networks. We will show comparisons to surface data from OpenAQ (https://openaq.org/) and the Sahelian Dust Transect (Marticorena et al., 2010) network, but will mainly rely on satellite and Aerosol Robotic Network (AERONET) observations. We use the column aerosol optical depth observations (AOD) from MODIS Collection 6 Terra Level 3 (Platnick et al. 2015) and from AERONET (Holben et al., 1998), and aerosol extinction profiles from CALIOP (Cloud-Aerosol Lidar with Orthogonal Polarization) Layer Product 3.0 (Winker et al., 2009). CALIOP profiles have been averaged here as described in (Koffi et al., 2012; 2016). As these observations provide information about aerosol column loads and height profiles, with less reliable information close to the surface, we use in addition the NASA Goddard Earth Observing System, version 5 (GEOS-5) model (Rienecker et al 2008), as a reference for surface simulated $PM_{2.5}$. Here we use the GEOS-5 model, with horizontal resolution of 0.5° × 0.625° in latitude and longitude, including the GOddard Chemistry Aerosol Radiation and Transport (GOCART) Model (Chin et al., 2000; Colarco et al., 2010) and the MERRA aerosol and meteorology data assimilation

Randels et al. 2017.

We chose the year 2016 for this study, as more AERONET data are available from the ObseRvations of Aerosols above CLouds and their intEractionS (ORACLES) field campaign (https://espo.nasa.gov/oracles/content/ORACLES) and the available GEOS-5 simulation. However, as a caveat the CMIP6 emissions only go until the year 2015, in years thereafter, perpetual 2015 biomass burning and anthropogenic emissions are used. This is not an issue for interactive emission sources such as dust, as nudged winds are available for all simulated years.

All data products are used on their original grids, and monthly mean values are used as released by the data product. If any other averaging is applied it will be explicitly stated.

Figure 1 displays AOD from MODIS Terra, AERONET and GISS-E2.1-MATRIX over Africa for the four seasons in 2016. Note that dust over land is mostly screened out in the standard MODIS retrievals due to remote sensing high signal to noise ratios over bright targets such as the Saharan desert, the same spatial screening is applied to the model. The model AOD includes dust, as aerosols are simulated as internally mixed particles, while MODIS Terra over land mostly excludes dust. The main large-scale aerosol features in Sub-Saharan Africa are the November to January biomass burning season in Western Africa, the June to September biomass-burning season in Angola, Congo and Zambia, and the Saharan dust season especially pronounced between May to August. The MODIS AOD retrieval off the coast of Angola is challenged, due to screening of the stable strati-form cloud deck over the ocean in the JJA and SON season. MODIS strongly overestimates AOD over the ocean during the burning seasons. Overall the model properly simulates the high burning seasons of DJF and JJA, but it underestimates the central African plume in the shoulder seasons. The statistical analysis performed with the monthly mean MODIS and model data over all African land points where MODIS reported data, includes 14023 data points, show mean AOD values of 0.24 (model) and 0.26 (MODIS), standard deviation of 0.22 (model) and 0.24 (MODIS) and a correlation coefficient of 0.75.

The AERONET observations are overlaid in Figure 1 and shown as time series in Figure 2. The arrival of the JJA biomass burning plume is well simulated as evident from the two stations on Ascension Island. The same feature, but on land, can be seen at Henties Bay (Namibia) and Namibe (Angola). Those stations similar to Ascension only capture the edge of the biomass burning plume. These stations can help to evaluate the correct timing of the burning, as well as plume transport. Ilorin (Nigeria) and Kofiridua (Ghana) are located closer to the biomass burning event, but still not in its center. Skzukuza and Upington show AOD in Southern Africa. Overall the model never underestimates AOD levels, but overestimates AOD in high AOD regions compared to AERONET.

The CALIPSO extinction profiles, Figure 3, allow us to compare vertical aerosol distribution. The bias between model and observations is shown in the figure title. Profiles are shown for the 3 regions as indicated by the white boxes in Figure 1. Overall the model compares well with the extinction profiles, with the exception of the late harvest season in the biomass burning areas, similar to what we have seen compared to MODIS; the JJA biomass burning is not extended enough into the SON season. The general overestimation as detected against AERONET is not visible here.

Translating AOD into surface concentrations, the measure needed for health impact studies, is difficult to do with CALIPSO due to degraded precision of the lidar signal close to the surface. To bridge this gap, we utilize a GEOS-5 simulation, which in terms of $PM_{2.5}$, is an additional model simulation. GEOS-5 uses assimilated weather and column AOD concentrations. The models are compared for August and September, during which the South Hemispheric biomass burning is strongest. The GEOS-5 model shows similar $PM_{2.5}$ levels to those simulated by GISS-E2.1-MATRIX (Figure 4), including urban plumes like air pollution in Lagos, Nigeria, and Johannesburg, South Africa. The modeled $PM_{2.5}$ is similar in magnitude to the one resolved by GEOS-5, but is not in the exact same location. This is due to a slight mismatch between fire locations in GEOS-5 (based on QFED (Darmenov et al 2015)) and in GISS-E2.1-MATRIX (based on GFED4s emissions (van Marle et al., 2017)). On an annual basis the GISS-E2.1-MATRIX (see Figure 7) shows very similar $PM_{2.5}$ concentrations over South Africa, compared to the regional study by (Garland, 2017), with values of about 15 $\mu g/m^3$ over Johannesburg and 2 – 6 $\mu g/m^3$ in remote areas.

In Figure 5, $PM_{2.5}$ station and model data are shown for the year 2017, as data coverage for 2016 was even less. Out of the entire OpenAQ database only three stations reported data for Africa, and two stations are located in the same city, Addis Ababa. The bias between model and station data ranges between -7.6 to 5.8 $\mu g/m^3$. The annual cycle in Addis Ababa is driven by dust, whereas Kampala has equal anthropogenic and natural (mainly dust) contributions to $PM_{2.5}$. Another set of station data measuring particle mass including larger particles, PM_{10}, is available for the Sahel. Figure 6 shows year 2016 and at one station 2014 concentrations. The model captures the stations in Senegal and Niger very well, while it strongly overestimates concentrations at the station in Mali. Natural aerosols are the main contributor to aerosol mass at those stations and anthropogenic aerosols peak from January to March.

Ozone and its precursors are not evaluated in this paper, but have been evaluated against the Tropospheric Emission Spectrometer (TES) instrument (Osterman et al., 2008) and the Southern Hemisphere Additional Ozone Sondes (SHADOZ) network (Thompson et al., 2007) for the GISS model (Shindell et al., 2013). Ozone and CO concentrations in the lower troposphere are very similar in our simulation compared to the ones evaluated in (Shindell et al., 2013).

4. Results

4.1 Air Pollution Simulation

The results of the air pollution simulation are displayed in Figure 7 for the concentrations of $PM_{2.5}$, O_3, SO_2 and CO, and they are segregated by their source: natural, industrial/domestic and biomass burning emissions, respectively. In the following discussion, the descriptions "natural", "industrial/domestic" and "biomass burning" are used. "Natural" refers to simulations in which the model only computes emission fluxes from natural sources, such as mineral desert dust, oceanic emissions of sea spray and DMS, emission fluxes from soils and vegetation, and lighting NO_x.

However, the "natural" results for the African continent are completely dominated by mineral desert dust. The "industrial/domestic" experiments account for sources such as industrial production, energy generation, transportation emissions, household emissions (other than fires) all taken from the CMIP6 emission inventory. The "biomass burning" experiment accounts for all fire emissions, whether they are of anthropogenic or natural origin, based on GFED4s. Note that we prefer not to name any of these experiments anthropogenic, as the fire emissions are not clearly segregated between its human and natural causes. That said, the overwhelming majority of fire emissions in Sub-Saharan Africa are caused by agricultural burning (Archibald et al., 2012), thus before we are able to draw more precise distinction we might consider both the "industrial/domestic" and "biomass burning" experiments as anthropogenic.

The model simulations are designed to include internal variability that is caused by the disturbance of an emission source and its impact via meteorological feedbacks on all other composition fields, including the emissions of the interactively computed sources, mainly desert dust, and to a smaller extend, DMS and sea salt. Because of internal feedbacks the numbers of the individual source experiments do not linearly add up to the total amount. The strongest sensitivities appear between anthropogenic and natural emissions. Removing anthropogenic emissions from the simulation leads to dryer surface conditions and enhances dust concentrations (Figure 7, first and second map). The reduced surface wetness is caused by less aerosol load in Central and West Africa, due to the removed anthropogenic emissions, including biomass burning. Fewer aerosols leads to reduced cloud droplet number concentrations and aerosol light extinction in the column. Eventually, reduced aerosol direct and indirect effects, lead to more shortwave radiation reaching the Earth surface in the 'natural' simulation. On an annual mean basis this leads to a reduction of surface humidity between 5 – 10% in the region around the Sahel and the Southern part of the Sahara and promoting more favorable conditions for dust storms.

Air pollution in the form of $PM_{2.5}$ on the African continent is dominated by the contribution of Saharan dust, that reaches in some seasons deep into West Africa. These dust storm and regional transport features matter for health impact studies. As in our case, high dust concentrations mix with local pollution and hits densely populated countries in West Africa, especially Nigeria. "Industrial/Domestic" $PM_{2.5}$ (Figure 7, first row, third plot) is explained by the large industrial centers, most visibly, Lagos in Nigeria, Johannesburg in South Africa, Addis Ababa in Ethiopia, and the industrial centers around Lake Victoria, spreading over multiple countries, including Kenya and Uganda. In addition, air pollution transported to Northern Africa from Europe is responsible for the enhanced $PM_{2.5}$, dominated by sulfate in that experiment, and ozone concentrations in the Sahara. 'Biomass burning' dominates over Central and West Africa, causing some feedbacks with dust emissions in the Sahara as previously discussed.

Near surface ozone pollution shows a very different pattern than $PM_{2.5}$. The large-scale ozone pattern is explained by biomass burning and "Industrial/domestic" sources in Europe and West Asia that long-range transport air pollution into Northern Africa. SO_2 contribution is dominated by the "Industrial/domestic" sector, and of all pollutants, it shows more local influences and less regional structures. CO, on the other hand, is dominated by the biomass burning sector and the four major industrial centers in Africa, that have been listed above for their contributions to $PM_{2.5}$.

Aerosols and gases, especially ozone, show very different responses to the investigated sectors on a regional basis. Understanding these differences are a prerequisite for our discussion on health impacts.

4.2 Health Impact Assessment

The numbers of premature deaths as calculated by the EVA system for the base case and the scenarios for the African continent as well as for fore sub-regions. Region R1, R2 and R3 are marked in Figure 1 (last map) and R4 is Africa south of 15°N. As seen in Table 2, the total number of premature deaths due to air pollution on the African continent in 2016 is calculated to be ~780,000. Out of these 780,000 premature deaths, ~715,000 (92%) were due to $PM_{2.5}$. Natural sources were responsible for ~550,000 premature deaths, accounting for ~71% of all premature deaths. $PM_{2.5}$ was responsible for 82% of the natural contribution to premature deaths in Africa. Anthropogenic emissions were responsible for ~180,000 premature deaths (~23%). Biomass burning was calculated to be responsible for ~43,000 premature deaths (~5%).

In the R4 region, the total number of premature deaths were calculated to be ~560,000 (Table 2). R4, mostly covering Sub-Saharan Africa, has the largest population density, hosting about 80% of the total population in Africa. The natural pollution contribution is ~67%, while anthropogenic sources were responsible for 25% and biomass burning responsible for 8%. The total number of premature deaths in West Africa was calculated to be ~105,000 (Table 2), where 42% were due to natural sources, 42% due to anthropogenic sources and 17% due to biomass burning. The highest contribution of $PM_{2.5}$ were calculated to be in West Africa (~74%), where the GISS-E2.1-MATRIX model also simulated the highest annual mean $PM_{2.5}$ concentrations among the sub regions (~20 μgm^{-3}). In Central Africa, air pollution was found to be responsible for ~25,000 premature deaths (Table 2), ~67% of which was attributed to $PM_{2.5}$. The natural sources were responsible for less than 1% of the total number of premature deaths, while the anthropogenic sources accounted for ~44% of the cases. Biomass burning had the largest contribution in comparison with other subregions, and it is responsible for 56% of premature deaths. Ozone levels were also calculated to be the highest among all the sub regions in Central Africa (annual mean of ~38 ppb). Finally, for South Africa, we have calculated the lowest number of premature deaths (~17,000: Table 2), where 77% were attributed to anthropogenic sources. This low number was due to lowest $PM_{2.5}$ (~6 μgm^{-3}) and ozone levels (15 ppb) calculated by the GISS-E2.1-MATRIX model, as well as the lowest population density. Natural sources and biomass burning only accounted for less than 1% and 11% of the cases, respectively. Anthropogenic emissions are calculated to be responsible for 89% of the premature deaths in South Africa.

Table 2 Premature deaths by region and experiment, brackets show 95% confidence level.

	Total	Natural	Industrial/Domestic	Biomass Burning
Africa	782 248 [766 043 - 797 716]	556 475 [544 948 - 567 479]	182 398 [178 619 - 186 004]	43 374 [42 476 - 44 232]
Sub-Sahara	563 218	378 403	136 798	39 036

below 15°N (R4)	[551 954 – 574 482]	[370 835 - 385 971]	[134 062 - 139 533]	[38 255 - 39 816]
West Africa (R1)	104 865 [102 693 - 106 939]	43 489 [42 588 - 44 349]	43 433 [42 533 - 44 292]	17 944 [17 572 - 18 298]
Central Africa (R2)	25 459 [24 932 - 25 963]	18 [17 - 18]	11 154 [10 923 - 11 375]	14 288 [13 992 - 14 570]
Southern Africa (R3)	17 085 [16 731 - 17 423]	27 [26 - 27]	15 165 [14 850 - 15 464]	1 893 [1 854 - 1 931]

The spatial distributions of premature deaths from acute and chronic exposure from natural, anthropogenic and biomass burning emissions are presented in Figure 8. The spatial distributions of premature deaths from natural and anthropogenic emissions are very similar, following the spatial distribution of $PM_{2.5}$, shown in Figure 8. Major cities in Nigeria and South Africa also stand out. Premature death due to biomass burning is concentrated over the sub Saharan region, following the high biomass burning $PM_{2.5}$ levels presented in Figure 7.

5. Discussion

According to the latest cause-specific mortality estimates for 2016 from the World Health Organization (2018), lower respiratory infection is the leading cause of death on the African continent (917,000 death per year). It became the leading cause of death in Africa over HIV/AIDS (719,000) since 2015, and it is the top deadly communicable disease worldwide. Compared to these data, our study suggests that outdoor air pollution is one of the leading causes of premature mortality in Africa. A caveat of our study is that indoor air pollution is not considered in this analysis, and its impact on health may be as large or even larger than outdoor pollution. A report by IHME (2015) found the rising impact of household air pollution on premature deaths in Africa. Total annual deaths from ambient particulate matter pollution across the African continent increased by 36% from 1990 to 2013, from a 180,000 in 1990 to 250,000 in 2013. Over this period, deaths from household air pollution also continued to increase, by 18%, from an already high base of 400,000 in 1990 to well over 450,000 in 2013 (IHME, 2015).

One motivation for this study was that the practice of agricultural burning creates one of the largest biomass burning events on Earth, easily detectable from space. We found that 43,000 premature deaths were caused by this practice, most of them in Sub-Saharan Africa. The number is relatively low, compared to other sub-regions and sectors. This is because this region is less densely populated and biomass aerosol plumes often peak away from the surface layer in the mid troposphere, as seen in Figure 3, and thus have a smaller health effect. Nevertheless, this type of land management, agricultural burning, is unsustainable, ecologically damaging and could be avoided by implementing improved land agricultural practices. At the same time, the affected countries are already struggling with extreme poverty rates, human rights violations and unstable political systems. Yet, even under these extremely challenging circumstances, air quality and public health should not be neglected.

Mineral desert dust is of overwhelming importance for public health in Africa. As discussed below it is not clear yet, whether dust minerals are as toxic as other chemical components of air pollution. We did not distinguish between different potential toxicity levels, but our model simulates

internally mixed aerosol composition. As in reality, aerosols are not comprised of one chemical component, but mixed through microphysical processes, such as condensation and coagulation. This effect makes it even harder to assign toxicity to an individual aerosol type. Further research is needed to investigate scenarios using fewer toxic assumptions for mineral components in our model, which will significantly change the mortality rates calculated here. On the other hand, we have not considered anthropogenic emissions of dust, which would possibly increase mortality rates again. For instance, cattle grazing and land conversion raise ecological concern in Africa (Jayne et al., 2014), and they can lead to new anthropogenic sources of dust.

Aerosols dominate the ambient pollution-related mortality over gases due to their complex composition of organic and inorganic components and sizes. They are a mixture of solid, liquid, or solid and liquid particles suspended in the air. These suspended particles vary in size, composition and origin. Therefore, their health impacts vary on their sizes, composition, and origin. Current health assessments of aerosols assume that all fine fraction particles affect health to a similar degree independent of origin, age and chemical composition of the particles. WHO (2013b) and (Lippmann, 2014) conclude that the cardiovascular effects of ambient $PM_{2.5}$ are greatly influenced by their transition metal contents and that even low concentrations of trace metals can be influential on health related responses. However, only few studies focus on individual particulate species, mainly black carbon and carbonaceous particles. In addition to PM, studies on human populations have not been able to isolate potential effects of NO_2, because of its complex link to aerosols and O_3.

Modeling Uncertainties

A full investigation of modeling uncertainties is beyond the scope of this paper, but other studies have investigated uncertainty ranges and we assume that similar ranges will apply to our study. Each step of modeling air pollution health studies, from emissions, to composition modeling and the health analysis, bears a margin of error. Starting with the emissions, large differences in bottom-up anthropogenic emissions estimates for Africa have been found when compared to satellite observations (Marais and Wiedinmyer, 2016). In this paper, we found that the biomass burning plume does not extend enough into the end of the season, and the locations of the burning differs between satellite, GEOS-5 and our model simulations, a bias that most likely is caused by the biomass emission inventory. Wildfire O_3 production also adds to the uncertainty of health studies. (Jaffe and Wigder, 2012) found that wildfire O_3 production is rather uncertain, due to the net effect of aerosols on chemical and photochemical reactions within a fire plume, the impact of oxygenated volatile organic compounds, as well as nitrous acid on O_3 production, and the interplay of variables that lead to extreme $\Delta O_3/\Delta CO$ values.

(Seltzer et al., 2017) evaluated the GISS model regarding metrics for human health for the United States and China. They found that results for O_3- and $PM_{2.5}$-based metrics featured minor differences due to the model resolutions and that model, meteorology, and emissions inventory each played larger roles in variances. Surface metrics related to O_3 were consistently high biased, though to varying degrees, demonstrating the need to evaluate particular modeling frameworks before O_3 impacts are quantified. Thus, the coarse model resolution of the GISS model did not show a systematic bias for health studies. Similar results related to model resolution using the

GEOS-Chem model on $PM_{2.5}$ and ozone concentration were found by (Li et al., 2016; Yu et al., 2016). (Li et al., 2016) compared a fine (0.5×0.66°) and a coarse resolution of (2×2.5°), and they found an 8% lower mortality rate for the US when using the finer model resolution.

Our aerosol evaluation did not show a systematic bias in the models simulated composition. The limited surface network observations in Africa make it impossible to estimate large scale biases and to include this into an uncertainty calculation. In a global study, (Shindell et al., 2018) concluded that model biases are shown to nearly always play a smaller role than uncertainties related to health effects. Another level of uncertainty is introduced by the country-level health statistics, pollution exposure response functions and the use of a concentration threshold. In this study using the EVA model, the number of premature deaths is calculated using the relative risk of 1.062 (1.040–1.083) on a 95 % confidence interval from (Pope et al., 2002) for all-cause mortality.

Toxicity of Gases and Aerosols

The health impact of aerosols is a function of aerosol composition, size, and concentration, as well as the individual's exposure time, genetics, and health condition. The respiratory system, skin, and eyes are organs sensitive to exposure. However, recent studies have also indicated the nervous system as sensitive to air pollution through exposure from inhalation and deposition (e.g. (Bos et al., 2014)). Deposition and thus exposure are controlled by size. The adverse effects of ultrafine particles are linked to their ability to gain access to the lung and systemic circulation (Nel, 2005) causing cardiovascular (Shah et al., 2013) and cancer diseases (Raaschou-Nielsen et al., 2013). Soluble particles may dissolve and pass through the skin or eyes, in which case size plays a relative minor role. Saharan dust mainly consists of clay minerals, quartz, calcium, and magnesium carbonates (Afeti and Resch, 2000). According to (West et al., 2016), recent studies have shown that combustion related aerosols are more toxic than bulk $PM_{2.5}$ mass, including components such as sulfates and nitrates. However, a literature review by (Wyzga and Rohr, 2015) found that none showed unequivocal evidence of zero health impact and that the carbon-containing PM appears to be most strongly associated with health effects. Several studies mention adverse health effects of the cardiorespiratory system that are associated with dust, but very few present quantitative results (De Longueville et al., 2010). These studies mainly examine short-term health effects based on time-series analysis. (Cook et al., 2007) considers dust the least toxic aerosol constituent. However, aerosol toxicity is hard to estimate, due to the fact that all aerosols are mixtures and not pure compounds and the body's response to a combination of pollutants may have synergistic or nonlinear impacts (West et al., 2016). Dust in particular may have a toxic effect by providing a surface for chemical reactions (e.g enhancing toxicity by allowing reactions like PAH->NPAH (Kameda et al., 2016)), by carrying fungus (e.g. valley fever), and through toxic metals (e.g. transition metals such as iron, or heavy metals such as lead, and arsenic).

It has been found that short-term exposure to O_3 can have independent effect on pulmonary function, lung inflammation, lung permeability, respiratory symptoms, increased medication usage, morbidity, and mortality, especially in the summer (WHO, 2003). There are also a number of studies showing that short-term effects of O_3 can be enhanced by particulate matter (e.g. (Gilliland et al., 2001)). Experimental evidence from studies at higher O_3 concentrations shows synergistic,

additive or antagonistic effects, depending on the experimental design, but their relevance for ambient exposures is unclear. O_3 also may act as a primer for allergen response.

The toxicity of chemical components of $PM_{2.5}$ in different parts of the world are not necessarily the same. A critical assumption in this work is that the exposure response functions used for calculating different morbidity and mortality outcomes are developed in Europe or in the U.S., where the ambient air pollutant levels and composition as well as the population response to these pollutants could be very different from Africa. Epidemiological studies targeting mortality due to air pollution, and developing more representative exposure response functions, is still lacking in Africa.

How does this study compare to previous studies?

The global model study by (Lelieveld et al., 2015) concluded that for Africa 273,000 premature mortality for adults ≥30 years old and infants < 5 years old is caused by outdoor $PM_{2.5}$ and ozone pollution in 2010. Similar to our study they concluded that desert dust is the main contributor to air pollution mortality on the African continent. (Lacey et al., 2017) found that in Africa, ambient particulate matter concentrations at present-day anthropogenic activity contribute to 13 210 annual premature deaths. On the other hand (Heft-Neal et al., 2018) found that $PM_{2.5}$ concentrations led to 449,000 (95% confidence interval, 194,000–709,000) additional deaths of infants in 2015. (Giannadaki et al., 2014) only considered dust aerosols and estimated a global cardiopulmonary mortality of about 402,000 in 2005. The associated years of life lost are about 3.47 million per year, globally. Our global number (not discussed in this study) is 2.9 million for natural aerosol. In summary, our study lies in the middle range of what other studies have reported. We calculate about 3 times higher premature death rates compared to (Lelieveld et al., 2015), about 10 times higher mortality for the anthropogenic sector compared to (Lacey et al., 2017), but only 4% (2000 infant death (< 9 months) mortality due to $PM_{2.5}$) of the infant mortality as reported by (Heft-Neal et al., 2018).

6. Conclusion

This study draws the following conclusions:

- Air pollution in Africa leads to the premature death of about 800,000 people per year, with particulate matter ($PM_{2.5}$) causing 2/3 of the premature death; gaseous air pollutants, mainly ozone, are responsible for the rest. Air quality related deaths rank within the top leading causes of death, possibly more than HIV/AIDS, and contributing strongly to the number one reason of death, lower respiratory infections.
- African continent-wide, mineral desert dust is the main contributor to mortality, followed by 'industrial/domestic' emissions and biomass burning.
- In Sub-Saharan Africa, the majority of premature deaths is caused by particulate matter. Natural aerosols are the largest contributor to air pollution, followed by anthropogenic pollution, which includes industrial, domestic, and agricultural.
- Biomass burning, mainly from agriculture, is responsible for half of premature deaths in Central Africa, with ozone as an important contributor, since its concentrations are highest there, compared to the other sub-regions selected in this study.

- South Africa is clearly dominated by the industrial and domestic sector, leading to 15,000 premature deaths.

We cannot stress the discussion about uncertainties enough when quantifying health impacts of air pollution. Thus, it is helpful to investigate this problem with different techniques. This study, a global modeling study based on satellite data evaluation, has the advantage to be applied anywhere in the world, including regions where no in-situ measurements are available. Further, it tests the usefulness of combining climate models with a health impact model, which can be applied to calculate health risk of past and future scenarios and link global health concerns with climate change.

Acknowledgement

We want to thank Dr. Karla Maria Longo De Freitas from GSFC for providing the GEOS-5 simulations. The authors acknowledge funding from NASA's Atmospheric Composition Modeling and Analysis Program (ACMAP), contract number NNX15AE36G. Resources supporting this work were provided by the NASA High-End Computing (HEC) Program through the NASA Center for Climate Simulation (NCCS) at Goddard Space Flight Center. Aarhus University gratefully acknowledges the NordicWelfAir project funded by the NordForsk's Nordic Programme on Health and Welfare (grant agreement no. 75007) and the REEEM project funded by the H2020-LCE Research and Innovation Action (grant agreement no.: 691739). The models simulated $PM_{2.5}$, ozone and health statistic data are available at data.giss.nasa.gov.

Figures

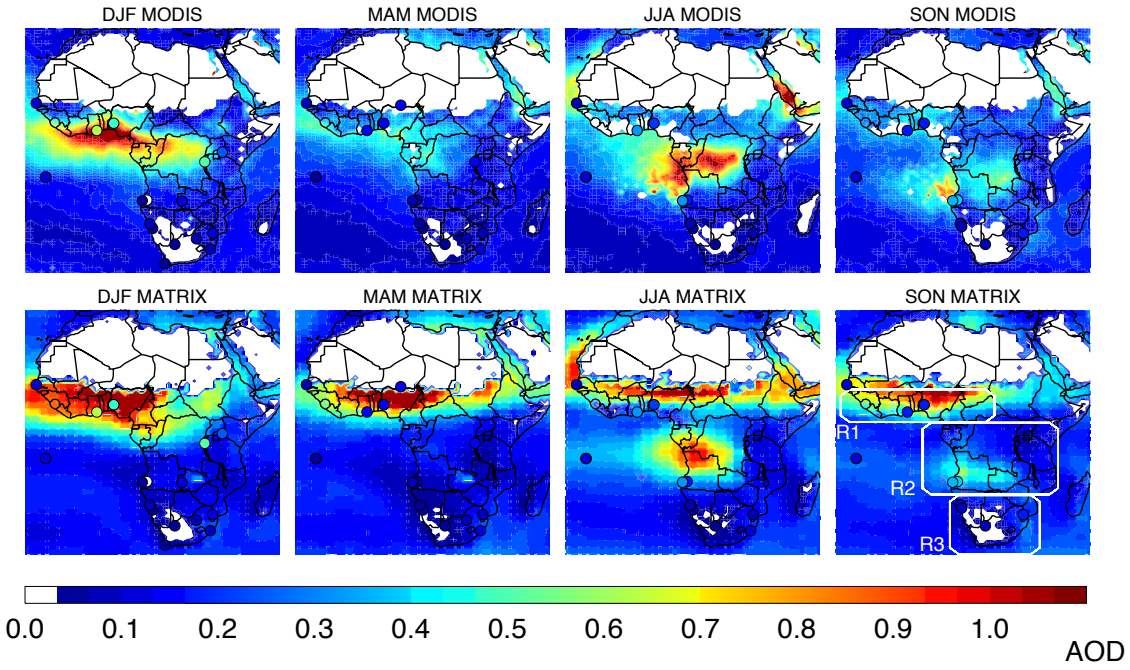

Figure 1: Maps of aerosol optical thickness for the four seasons in 2016 shown for MODIS Terra (upper) and GISS-E2.1-MATRIX (lower panels). The model is sampled when satellite data are available. White areas have no data coverage. Seasonally averaged AERONET measurements are shown in the filled circles. The white borders on the last map indicate the sub regions used in this paper.

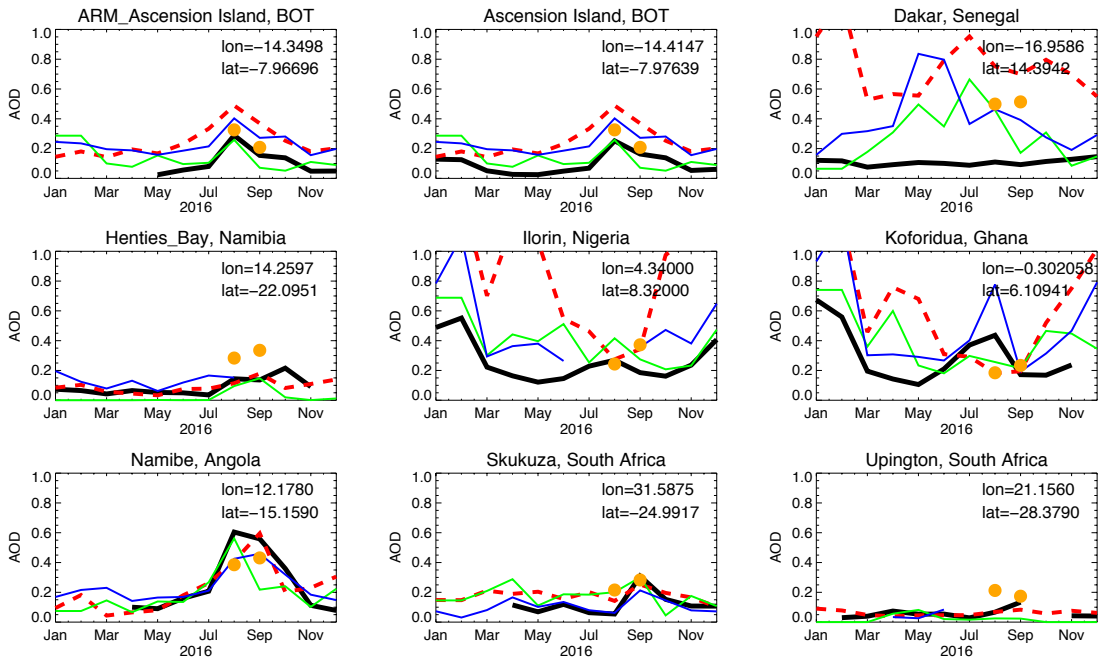

585

586 Figure 2 Time series of column optical thickness at 9 stations. AERONET (black), GISS_E2.1-
587 MATRIX (red dashed), MODIS (green), CALIPSO (blue) and GEOS-5 (orange dots).

588

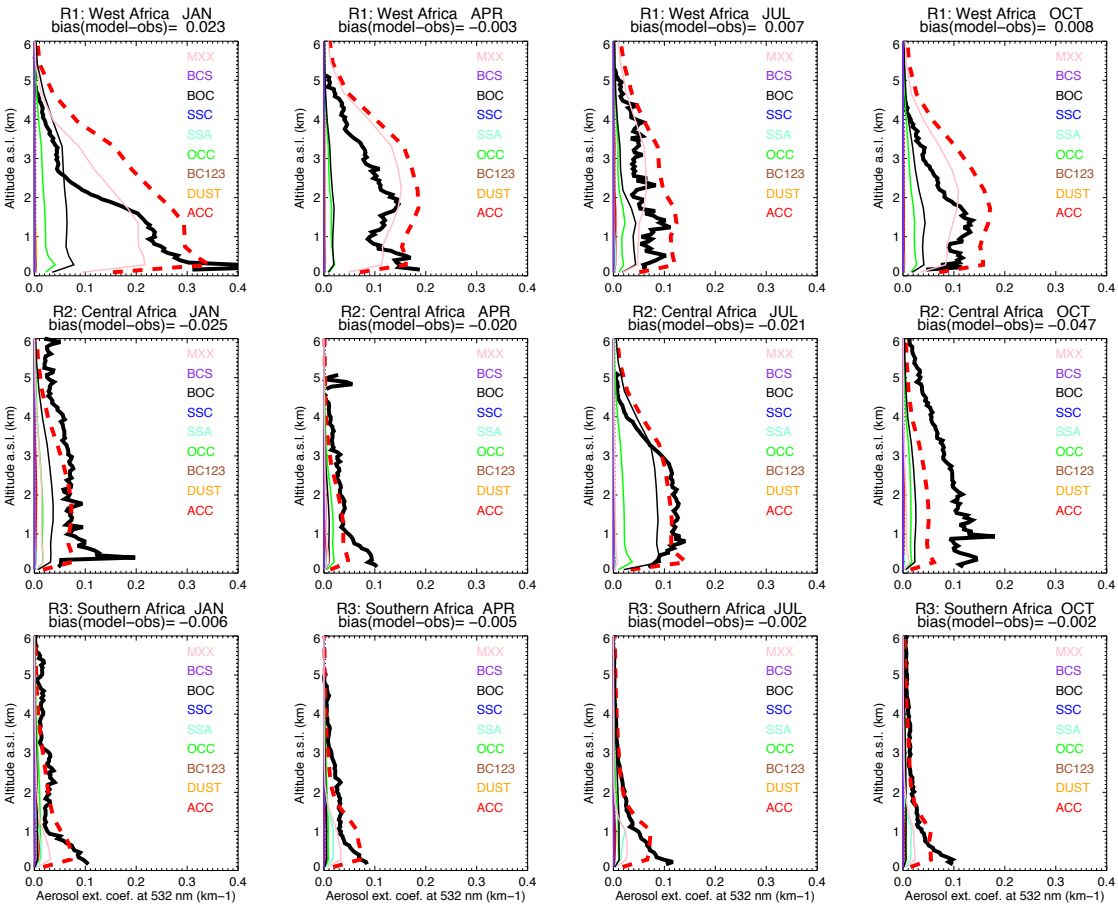

Figure 3 Height profile plots of aerosol extinction. For the areas as indicated in Figure 1.: R1, West Africa (first row), R2 Central Africa (second row) and R3 Southern Africa (third row). CALIPSO profiles (black) and GISS-E2.1-MARIX (dashed red total), individual colors (see legend) show contribution by aerosol population towards the total profiles are shown. The most dominant populations are, black and organic carbon mixtures including inorganic coatings (BOC, thin black line), organic carbon with inorganic coatings (OCC, thin green line), and dust containing mixing states (MXX, thin pink line). See Table 1a in Bauer at al 2008 for explanation of all mixing state classes. The column mean aerosol extinction bias between model and observations is shown in the title.

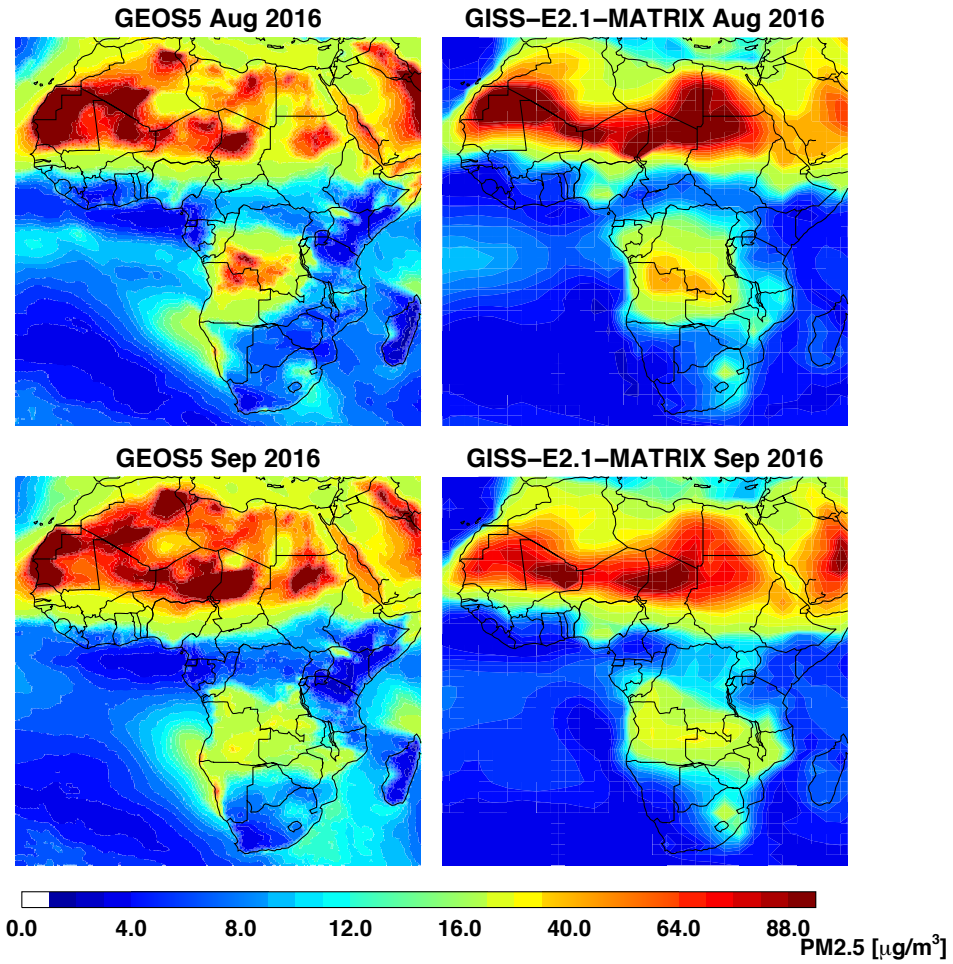

603
604
605 Figure 4 $PM_{2.5}$ concentrations for August (upper) and September (lower panels) 2016 shown for
606 GEOS-5 and GISS-E2.1-MATRIX.
607

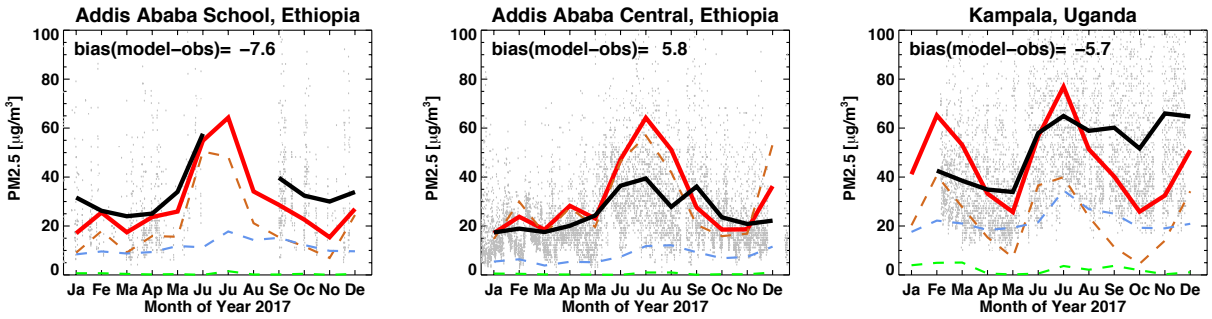

Figure 5 Time series of surface $PM_{2.5}$ concentrations for the year 2017. Measurements from the US Diplomatic Posts in Addis Ababa and Kampala, hourly data in grey and monthly averaged in black, are compared to the monthly mean model data, red solid line. The dashed lines show the contribution of anthropogenic (blue), natural (brown) and biomass burning (green) sources to the modeled $PM_{2.5}$. The bias is the difference between annual mean modeled and measured $PM_{2.5}$.

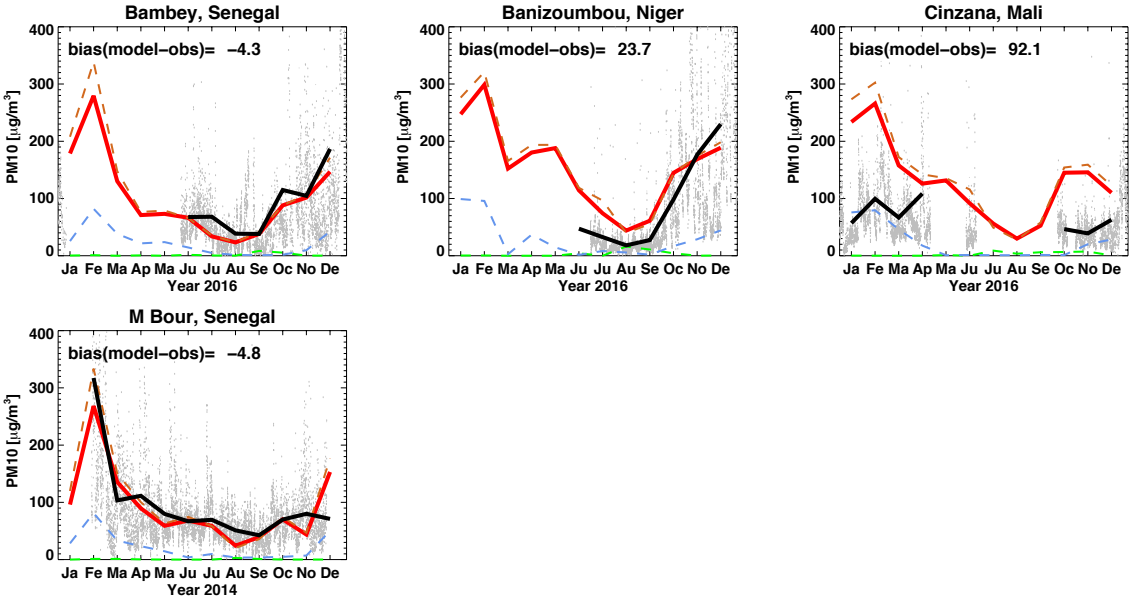

Figure 6 Time series of surface PM_{10} concentrations for year 2016 (upper panel) and 2014 (lower panel). Measurements from the Sahelian Dust Transect stations, hourly data in grey and monthly averaged in black, are compared to the monthly mean model data, red solid line. The dashed lines show the contribution of anthropogenic (blue), natural (brown) and biomass burning (green) sources to the modeled PM_{10}. The bias is the difference between annual mean modeled and measured PM_{10}.

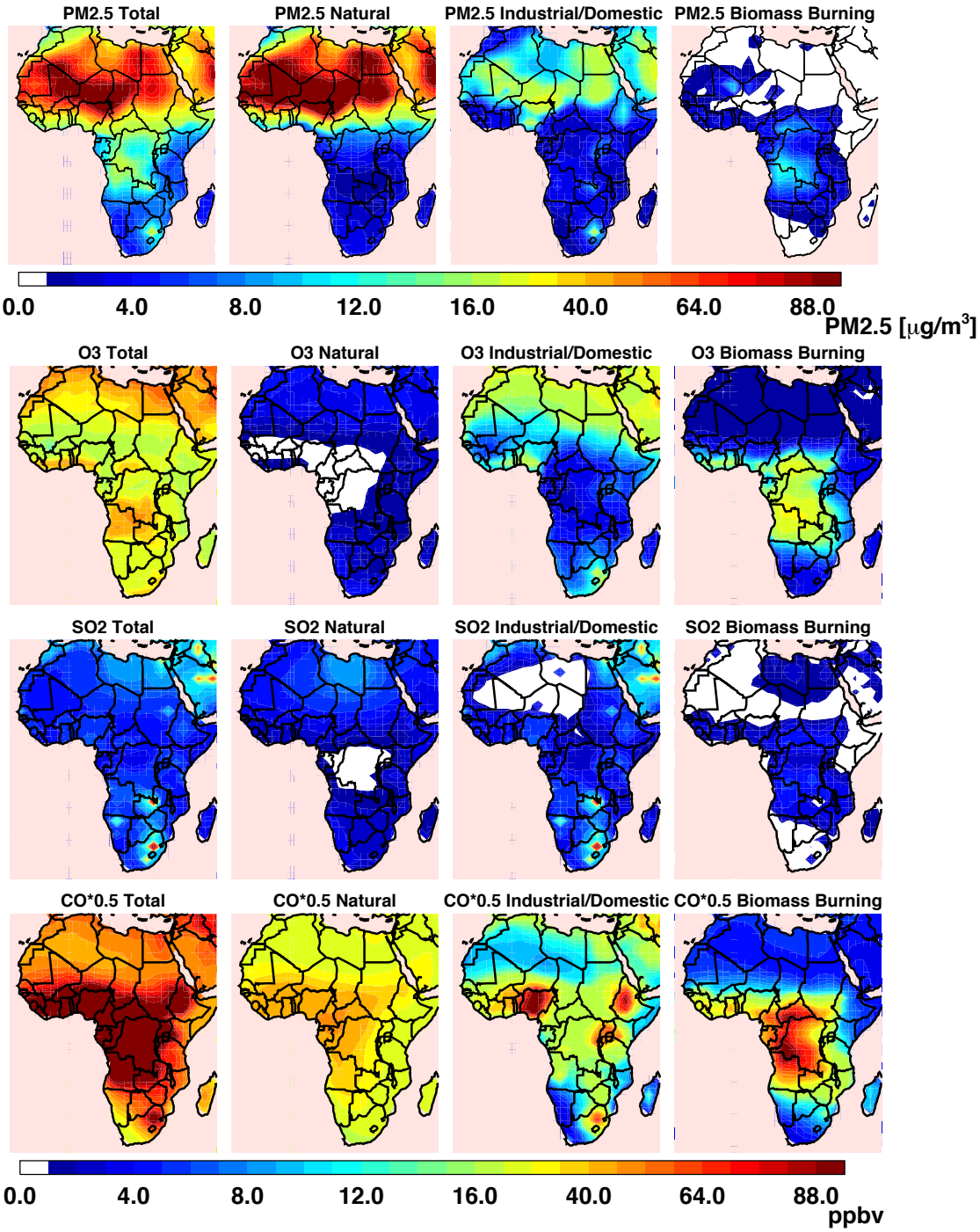

Figure 7 Surface annual mean $PM_{2.5}$ (μg/m3) (upper panels), ozone (second row), SO_2 (third row) and CO (lower panels, divided by 2 to fit color scale) concentrations (ppb_v) for 2016. Total concentrations are displayed in first column, and its natural, industrial/domestic and biomass burning contributions in the subsequent columns.

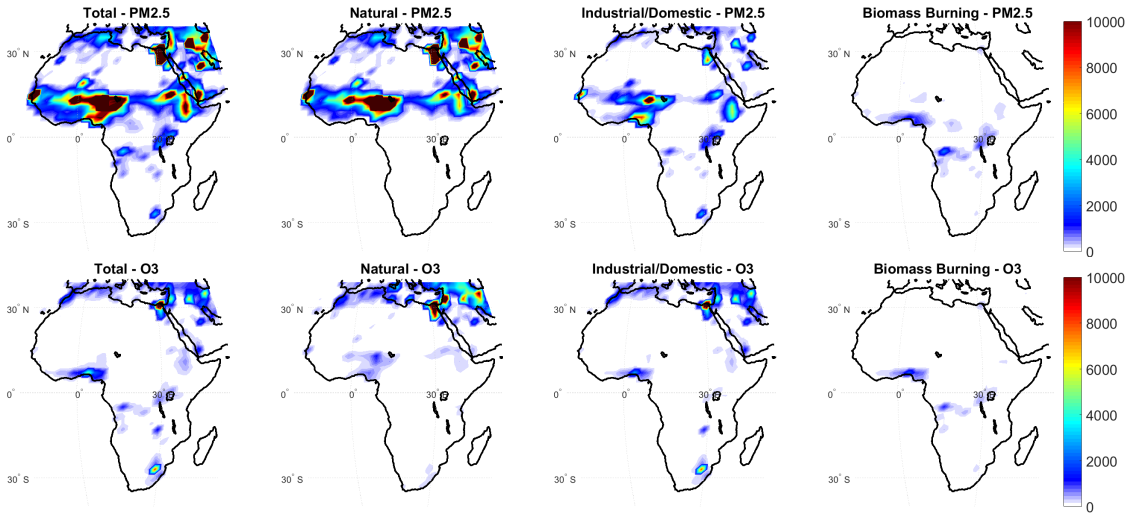

Figure 8 Premature death due to $PM_{2.5}$ (upper) and ozone (lower panel). The first column shows the total, followed by separate contributions by emission sources, natural, industrial/domestic and biomass burning.

642 **References**
643

644 Afeti, G. M. and Resch, F. J.: Physical characteristics of Saharan dust near the Gulf of Guinea,
645 Atmospheric Environment, 34(8), 1273–1279, doi:10.1016/S1352-2310(99)00296-4, 2000.

646 Aghedo, A. M., Schultz, M. G. and Rast, S.: The influence of African air pollution on regional
647 and global tropospheric ozone, Atmospheric Chemistry and Physics, (7), 1193–1212, 2007.

648 Ahmed, R., Robinson, R. and Mortimer, K.: The epidemiology of noncommunicable respiratory
649 disease in sub-Saharan Africa, the Middle East, and North Africa, Mal. Med. J, 29(2), 203–9,
650 doi:10.4314/mmj.v29i2.24, 2017.

651 Amegah, A. K. and Agyei-Mensah, S.: Urban air pollution in Sub-Saharan Africa: Time for
652 action, Environmental Pollution, 220(Part A), 738–743, doi:10.1016/j.envpol.2016.09.042, 2017.

653 Archibald, S., Staver, A. C. and Levin, S. A.: Evolution of human-driven fire regimes in Africa,
654 Proceedings of the National Academy of Sciences, 109(3), 847–852,
655 doi:10.1073/pnas.1118648109, 2012.

656 Assamoi, E.-M. and Liousse, C.: A new inventory for two-wheel vehicle emissions in West
657 Africa for 2002, Atmospheric Environment, 44(32), 3985–3996,
658 doi:10.1016/j.atmosenv.2010.06.048, 2010.

659 Bauer, S. E., Ault, A. and Prather, K. A.: Evaluation of aerosol mixing state classes in the GISS-
660 modelE-MATRIX climate model using single particle mass spectrometry measurements, J.
661 Geophys. Res. Atmos., 118(17), n/a–n/a, doi:10.1002/jgrd.50700, 2013.

662 Bauer, S. E., Wright, D. L., Koch, D., Lewis, E. R., Mcgraw, R., Chang, L. S., Schwartz, S. E.
663 and Ruedy, R.: MATRIX (Multiconfiguration Aerosol TRacker of mIXing state): an aerosol
664 microphysical module for global atmospheric models, Atmospheric Chemistry and Physics,
665 8(20), 6003–6035, doi:10.5194/acp-8-6003-2008, 2008.

666 Bos, I., De Boever, P., Panis, L. I. and Meeusen, R.: Physical Activity, Air Pollution and the
667 Brain, Sports Med, 44(11), 1505–1518, doi:10.1007/s40279-014-0222-6, 2014.

668 Brandt, J., Silver, J. D., Christensen, J. H., Andersen, M. S., Bønløkke, J. H., Sigsgaard, T.,
669 Geels, C., Gross, A., Hansen, A. B., Hansen, K. M., Hedegaard, G. B., Kaas, E. and Frohn, L. M.:
670 Assessment of past, present and future health-cost externalities of air pollution in Europe and the
671 contribution from international ship traffic using the EVA model system, Atmospheric Chemistry
672 and Physics, 13(15), 7747–7764, doi:10.5194/acp-13-7747-2013, 2013a.

673 Brandt, J., Silver, J. D., Christensen, J. H., Andersen, M. S., Bønløkke, J. H., Sigsgaard, T.,
674 Geels, C., Gross, A., Hansen, A. B., Hansen, K. M., Hedegaard, G. B., Kaas, E. and Frohn, L. M.:
675 Contribution from the ten major emission sectors in Europe and Denmark to the health-cost
676 externalities of air pollution using the EVA model system – an integrated modelling approach,
677 Atmospheric Chemistry and Physics, 13(15), 7725–7746, doi:10.5194/acp-13-7725-2013, 2013b.

678 Cecil, D. J., Buechler, D. E. and Blakeslee, R. J.: Gridded lightning climatology from TRMM-
679 LIS and OTD: Dataset description, Atmospheric Research, 135-136, 404–414,
680 doi:10.1016/j.atmosres.2012.06.028, 2014.

Chin, M., Rood, R. B., Lin, S.-J., Müller, J. F. and Thompson, A. M.: Atmospheric sulfur cycle simulated in the global model GOCART: Model description and global properties, J. Geophys. Res. Atmos., 105(D20), 24671–24687, doi:10.1029/2000JD900384, 2000.

Christian, H. J., Blakeslee, R. J., Boccippio, D. J., Boeck, W. L., Buechler, D. E., Driscoll, K. T., Goodman, S. J., Hall, J. M., Koshak, W. J., Mach, D. M. and Stewart, M. F.: Global frequency and distribution of lightning as observed from space by the Optical Transient Detector, J. Geophys. Res. Atmos., 108(D1), ACL 4–1–ACL 4–15, doi:10.1029/2002JD002347, 2003.

Colarco, P., da Silva, A., Chin, M. and Diehl, T.: Online simulations of global aerosol distributions in the NASA GEOS-4 model and comparisons to satellite and ground-based aerosol optical depth, J. Geophys. Res. Atmos., 115(D14), D10S07, doi:10.1029/2009JD012820, 2010.

Cook, R. M., Andrew M Wilson, Jouni T Tuomisto, Oswaldo Morales, Marko Tainio, A.John S Evans: A Probabilistic Characterization of the Relationship between Fine Particulate Matter and Mortality: Elicitation of European Experts, Environ. Sci. Technol., 41(18), 6598–6605, doi:10.1021/es0714078, 2007.

De Longueville, F., Hountondji, Y.-C., Henry, S. and Ozer, P.: What do we know about effects of desert dust on air quality and human health in West Africa compared to other regions? Science of the Total Environment, The, 409(1), 1–8, doi:10.1016/j.scitotenv.2010.09.025, 2010.

EEA: Air quality in Europe, Technical report 5/2015, Copenhagen, European Environment Agency, 2015.

EEA: Road user charges for heavy goods vehicles: Tables with external costs of air pollution, Technical report 1/2013, Copen- hagen, European Environment Agency, 2013.

Evans, J., van Donkelaar, A., Martin, R. V., Burnett, R., Rainham, D. G., Birkett, N. J. and Krewski, D.: Estimates of global mortality attributable to particulate air pollution using satellite imagery, Environmental Research, 120, 33–42, doi:10.1016/j.envres.2012.08.005, 2013.

Forouzanfar, M. H., Alexander, L., Anderson, H. R., Bachman, V. F., Biryukov, S., Brauer, M., Burnett, R., Casey, D., Coates, M. M., Cohen, A., Delwiche, K., Estep, K., Frostad, J. J., KC, A., Kyu, H. H., Moradi-Lakeh, M., Ng, M., Slepak, E. L., Thomas, B. A., Wagner, J., Aasvang, G. M., Abbafati, C., Ozgoren, A. A., Abd-Allah, F., Abera, S. F., Aboyans, V., Abraham, B., Abraham, J. P., Abubakar, I., Abu-Rmeileh, N. M. E., Aburto, T. C., Achoki, T., Adelekan, A., Adofo, K., Adou, A. K., Adsuar, J. C., Afshin, A., Agardh, E. E., Khabouri, Al, M. J., Lami, Al, F. H., Alam, S. S., Alasfoor, D., Albittar, M. I., Alegretti, M. A., Aleman, A. V., Alemu, Z. A., Alfonso-Cristancho, R., Alhabib, S., Ali, R., Ali, M. K., Alla, F., Allebeck, P., Allen, P. J., Alsharif, U., Alvarez, E., Alvis-Guzman, N., Amankwaa, A. A., Amare, A. T., Ameh, E. A., Ameli, O., Amini, H., Ammar, W., Anderson, B. O., Antonio, C. A. T., Anwari, P., Cunningham, S. A., Arnlöv, J., Arsenijevic, V. S. A., Artaman, A., Asghar, R. J., Assadi, R., Atkins, L. S., Atkinson, C., Avila, M. A., Awuah, B., Badawi, A., Bahit, M. C., Bakfalouni, T., Balakrishnan, K., Balalla, S., Balu, R. K., Banerjee, A., Barber, R. M., Barker-Collo, S. L., Barquera, S., Barregard, L., Barrero, L. H., Barrientos-Gutierrez, T., Basto-Abreu, A. C., Basu, A., Basu, S., Basulaiman, M. O., Ruvalcaba, C. B., Beardsley, J., Bedi, N., Bekele, T., Bell, M. L., Benjet, C., Bennett, D. A., et al.: Global, regional, and national comparative risk assessment of 79 behavioural, environmental and occupational, and metabolic risks or clusters of risks in 188 countries, 1990–2013: a systematic analysis for the Global Burden of Disease Study 2013, The Lancet, 386(10010), 2287–2323, doi:10.1016/S0140-6736(15)00128-2, 2015.

724 Friedrich, R. and Bickel, P.: Environmental External Costs of Transport, Springer Science &
725 Business Media. 2001.

726 Garland, R. M.: Air quality indicators from the Environmental Performance Index: potential use
727 and limitations in South Africa, Clean Air Journal, 27(1), 33–41, doi:10.17159/2410-
728 972X/2017/v27n1a8, 2017.

729 Giannadaki, D., Pozzer, A. and Lelieveld, J.: Modeled global effects of airborne desert dust on air
730 quality and premature mortality, Atmospheric Chemistry and Physics, 14(2), 957–968,
731 doi:10.5194/acp-14-957-2014, 2014.

732 Giglio, L., Randerson, J. T. and van der werf, G. R.: Analysis of daily, monthly, and annual
733 burned area using the fourth-generation global fire emissions database (GFED4), Journal of
734 Geophysical Research: Biogeosciences, 118(1), 317–328, doi:10.1002/jgrg.20042, 2013.

735 Gilliland, F. D., Berhane, K., Rappaport, E. B., Epidemiology, D. T.2001: The Effects of
736 Ambient Air Pollution on School Absenteeism Due to Respiratory Illnesses, Epidemiology,
737 12(1), 43–54, doi:10.2307/3703678, 2001.

738 Goldammer, J. G. and Price, C.: Potential Impacts of Climate Change on Fire Regimes in the
739 Tropics Based on Magicc and a GISS GCM-Derived Lightning Model, Climatic Change, 39(2-3),
740 273–296, doi:10.1023/A:1005371923658, 1998.

741 Heft-Neal, S., Burney, J., Bendavid, E. and Burke, M.: Robust relationship between air quality
742 and infant mortality in Africa, Nature, 559(7713), 254–258, doi:10.1038/s41586-018-0263-3,
743 2018.

744 Hoesly, R. M., Smith, S. J., Feng, L., Klimont, Z., Janssens-Maenhout, G., Pitkanen, T., Seibert,
745 J. J., Vu, L., Andres, R. J., Bolt, R. M., Bond, T. C., Dawidowski, L., Kholod, N., Kurokawa, J.-
746 I., Li, M., Liu, L., Lu, Z., Moura, M. C. P., O amp apos Rourke, P. R. and Zhang, Q.: Historical
747 (1750–2014) anthropogenic emissions of reactive gases and aerosols from the Community
748 Emissions Data System (CEDS), Geosci. Model Dev., 11(1), 369–408, doi:10.5194/gmd-11-369-
749 2018, 2018.

750 Holben, B. N., Eck, T. F., Slutsker, I., Tanre, D., Buis, J. P., Setzer, A., Vermote, E., Reagan, J.
751 A., Kaufman, Y. J., Nakajima, T., Lavenu, F., Jankowiak, I. and Smirnov, A.: AERONET—A
752 Federated Instrument Network and Data Archive for Aerosol Characterization, Remote Sensing
753 of Environment, 66(1), 1–16, doi:10.1016/S0034-4257(98)00031-5, 1998.

754 IHME (2015), Global Burden of Disease Study 2013 (GBD 2013) – Results by Risk Factor –
755 Country Level (on line data base – Viz Hub –GBD Compare), Institute for Health Metrics and
756 Evaluation, University of Washington, Seattle, (http://vizhub.healthdata.org/gbd-compare/).

757 Im, U., Brandt, J., Geels, C., Hansen, K. M., Christensen, J. H., Andersen, M. S., Solazzo, E.,
758 Kioutsioukis, I., Alyuz, U., Balzarini, A., Baro, R., Bellasio, R., Bianconi, R., Bieser, J., Colette,
759 A., Curci, G., Farrow, A., Flemming, J., Fraser, A., Jimenez-Guerrero, P., Kitwiroon, N., Liang,
760 C.-K., Nopmongcol, U., Pirovano, G., Pozzoli, L., Prank, M., Rose, R., Sokhi, R., Tuccella, P.,
761 Unal, A., Vivanco, M. G., West, J., Yarwood, G., Hogrefe, C. and Galmarini, S.: Assessment and
762 economic valuation of air pollution impacts on human health over Europe and the United States
763 as calculated by a multi-model ensemble in the framework of AQMEII3, Atmospheric Chemistry
764 and Physics, 18(8), 5967–5989, doi:10.5194/acp-18-5967-2018, 2018.

765 Jaffe, D. A. and Wigder, N. L.: Ozone production from wildfires: A critical review, Atmospheric
766 Environment, 51, 1–10, doi:10.1016/j.atmosenv.2011.11.063, 2012.

767 Jayne, T. S., Chamberlin, J. and Headey, D. D.: Land pressures, the evolution of farming systems,
768 and development strategies in Africa: A synthesis, Food Policy, 48(C), 1–17,
769 doi:10.1016/j.foodpol.2014.05.014, 2014.

770 Kameda, T., Azumi, E., Fukushima, A., Tang, N., Matsuki, A., Kamiya, Y., Toriba, A. and
771 Hayakawa, K.: Mineral dust aerosols promote the formation of toxic nitropolycyclic aromatic
772 compounds, Scientific Reports 2016 6, 6(1), 24427, doi:10.1038/srep24427, 2016.

773 Katsouyanni, K., Touloumi, G., Spix, C., Schwartz, J., Balducci, F., Medina, S., Rossi, G.,
774 Wojtyniak, B., Sunyer, J., Bacharova, L., Schouten, J. P., Ponka, A. and Anderson, H. R.: Short
775 term effects of ambient sulphur dioxide and particulate matter on mortality in 12 European cities:
776 results from time series data from the APHEA project, BMJ, 314(7095), 1658–1658,
777 doi:10.1136/bmj.314.7095.1658, 1997.

778 Kim, D., Chen, Y., Camargo, S. J., Yao, M.-S., Nazarenko, L., Kin, D., Sobel, A. H., Del Genio,
779 A. D. and Kelley, M.: The Tropical Subseasonal Variability Simulated in the NASA GISS
780 General Circulation Model, http://dx.doi.org/10.1175/JCLI-D-11-00447.1, 25(13), 4641–4659,
781 doi:10.1175/JCLI-D-11-00447.1, 2012.

782 Knippertz, P., Fink, A. H., Deroubaix, A., Morris, E., Tocquer, F., Evans, M. J., Flamant, C.,
783 Gaetani, M., Lavaysse, C., Mari, C., Marsham, J. H., Meynadier, R., Affo-Dogo, A., Bahaga, T.,
784 Brosse, F., Deetz, K., Guebsi, R., Latifou, I., Maranan, M., Rosenberg, P. D. and Schlueter, A.: A
785 meteorological and chemical overview of the DACCIWA field campaign in West Africa in June–
786 July 2016, Atmospheric Chemistry and Physics, 17(17), 10893–10918, doi:10.5194/acp-17-
787 10893-2017, 2017.

788 Koffi, B., Schulz, M., Bréon, F. M., Griesfeller, J., Winker, D., Balkanski, Y., Bauer, S. E.,
789 Berntsen, T., Chin, M. A., Collins, W. D., Dentener, F., Diehl, T., Easter, R., Ghan, S., Ginoux,
790 P., Gong, S. L., Horowitz, L. W., Iversen, T., Kirkevag, A., Koch, D., Krol, M., Myhre, G., Stier,
791 P. and Takemura, T.: Application of the CALIOP layer product to evaluate the vertical
792 distribution of aerosols estimated by global models: AeroCom phase I results, J. Geophys. Res.,
793 117(D10), n/a–n/a, doi:10.1029/2011jd016858, 2012.

794 Koffi, B., Schulz, M., Bréon, F.-M., Dentener, F., Steensen, B. M., Griesfeller, J., Winker, D.,
795 Balkanski, Y., Bauer, S. E., Bellouin, N., Berntsen, T., Bian, H., Chin, M., Diehl, T., Easter, R.,
796 Ghan, S., Hauglustaine, D. A., Iversen, T., Kirkevåg, A., Liu, X., Lohmann, U., Myhre, G.,
797 Rasch, P., Seland, Ø., Skeie, R. B., Steenrod, S. D., Stier, P., Tackett, J., Takemura, T.,
798 Tsigaridis, K., Vuolo, M. R., Yoon, J. and Zhang, K.: Evaluation of the aerosol vertical
799 distribution in global aerosol models through comparison against CALIOP measurements:
800 AeroCom phase II results, J. Geophys. Res. Atmos., 121(12), 7254–7283,
801 doi:10.1002/2015JD024639, 2016.

802 Lacey, F. G., Marais, E. A., Henze, D. K., Lee, C. J., van Donkelaar, A., Martin, R. V., Hannigan,
803 M. P. and Wiedinmyer, C.: Improving present day and future estimates of anthropogenic sectoral
804 emissions and the resulting air quality impacts in Africa, Faraday Discussions, 200, 397–412,
805 doi:10.1039/C7FD00011A, 2017.

Lelieveld, J., Evans, J. S., Fnais, M., Giannadaki, D. and Pozzer, A.: The contribution of outdoor air pollution sources to premature mortality on a global scale, Nature, 525(7569), 367–371, doi:10.1038/nature15371, 2015.

Li, Y., Henze, D. K., Jack, D. and Kinney, P. L.: The influence of air quality model resolution on health impact assessment for fine particulate matter and its components, Air Qual Atmos Health, 9(1), 51–68, doi:10.1007/s11869-015-0321-z, 2016.

Liousse, C., Assamoi, E., Criqui, P., Granier, C. and Rosset, R.: Explosive growth in African combustion emissions from 2005 to 2030, Environ. Res. Lett., 9(3), 035003, doi:10.1088/1748-9326/9/3/035003, 2014.

Lippmann, M.: Toxicological and epidemiological studies of cardiovascular effects of ambient air fine particulate matter (PM2.5) and its chemical components: Coherence and public health implications, Critical Reviews in Toxicology, 44(4), 299–347, doi:10.3109/10408444.2013.861796, 2014.

Magi, B. I., Rabin, S., Shevliakova, E. and Pacala, S.: Separating agricultural and non-agricultural fire seasonality at regional scales, Biogeosciences, 9(8), 3003–3012, doi:10.5194/bg-9-3003-2012, 2012.

Marais, E. A. and Wiedinmyer, C.: Air Quality Impact of Diffuse and Inefficient Combustion Emissions in Africa (DICE-Africa), Environ. Sci. Technol., 50(19), 10739–10745, doi:10.1021/acs.est.6b02602, 2016.

Marticorena, B., Chatenet, B., Rajot, J. L., Traore, S., Coulibaly, M., Diallo, A., Kone, I., Maman, A., Diaye, T. N. and Zakou, A.: Temporal variability of mineral dust concentrations over West Africa: analyses of a pluriannual monitoring from the AMMA Sahelian Dust Transect, Atmospheric Chemistry and Physics, 10(18), 8899–8915, doi:10.5194/acp-10-8899-2010, 2010.

Miller, R. L., Schmidt, G. A., Nazarenko, L. S., Tausnev, N., Bauer, S. E., DelGenio, A. D., Kelley, M., Lo, K. K., Ruedy, R., Shindell, D. T., Aleinov, I., Bauer, M., Bleck, R., Canuto, V., Chen, Y., Cheng, Y., Clune, T. L., Faluvegi, G., Hansen, J. E., Healy, R. J., Kiang, N. Y., Koch, D., Lacis, A. A., LeGrande, A. N., Lerner, J., Menon, S., Oinas, V., Pérez García-Pando, C., Perlwitz, J. P., Puma, M. J., Rind, D., Romanou, A., Russell, G. L., Sato, M., Sun, S., Tsigaridis, K., Unger, N., Voulgarakis, A., Yao, M.-S. and Zhang, J.: CMIP5 historical simulations (1850-2012) with GISS ModelE2, J. Adv. Model. Earth Syst., 6(2), n/a–n/a, doi:10.1002/2013MS000266, 2014.

Murray, L. T.: Lightning NOx and Impacts on Air Quality, Curr Pollution Rep, 2(2), 115–133, doi:10.1007/s40726-016-0031-7, 2016.

Nel, A.: Air Pollution-Related Illness: Effects of Particles, Science, 308(5723), 804–806, doi:10.1126/science.1108752, 2005.

Osterman, G. B., Kulawik, S. S., Worden, H. M., Richards, N. A. D., Fisher, B. M., Eldering, A., Shephard, M. W., Froidevaux, L., Labow, G., Luo, M., Herman, R. L., Bowman, K. W. and Thompson, A. M.: Validation of Tropospheric Emission Spectrometer (TES) measurements of the total, stratospheric, and tropospheric column abundance of ozone, J. Geophys. Res., 113(D15), 1102–11, doi:10.1029/2007JD008801, 2008.

Petkova, E. P., Jack, D. W., Volavka-Close, N. H. and Kinney, P. L.: Particulate matter pollution in African cities, Air Qual Atmos Health, 6(3), 603–614, doi:10.1007/s11869-013-0199-6, 2013.

Platnick, S., et al., 2015. MODIS Atmosphere L3 Monthly Product. NASA MODIS Adaptive Processing System, Goddard Space Flight Center, USA: http://dx.doi.org/10.5067/MODIS/MOD08_M3.006

Pope, C. A., III, Burnett, R. T., Thun, M. J., Calle, E. E., Krewski, D., Ito, K. and Thurston, G. D.: Lung Cancer, Cardiopulmonary Mortality, and Long-term Exposure to Fine Particulate Air Pollution, JAMA, 287(9), 1132–1141, doi:10.1001/jama.287.9.1132, 2002.

Raaschou-Nielsen, O., Andersen, Z. J., Beelen, R., Samoli, E., Stafoggia, M., Weinmayr, G., Hoffmann, B., Fischer, P., Nieuwenhuijsen, M. J., Brunekreef, B., Xun, W. W., Katsouyanni, K., Dimakopoulou, K., Sommar, J., Forsberg, B., Modig, L., Oudin, A., Oftedal, B., Schwarze, P. E., Nafstad, P., De Faire, U., Pedersen, N. L., Östenson, C.-G., Fratiglioni, L., Penell, J., Korek, M., Pershagen, G., Eriksen, K. T., Sørensen, M., Tjønneland, A., Ellermann, T., Eeftens, M., Peeters, P. H., Meliefste, K., Wang, M., Bueno-de-Mesquita, B., Key, T. J., de Hoogh, K., Concin, H., Nagel, G., Vilier, A., Grioni, S., Krogh, V., Tsai, M.-Y., Ricceri, F., Sacerdote, C., Galassi, C., Migliore, E., Ranzi, A., Cesaroni, G., Badaloni, C., Forastiere, F., Tamayo, I., Amiano, P., Dorronsoro, M., Trichopoulou, A., Bamia, C., Vineis, P. and Hoek, G.: Air pollution and lung cancer incidence in 17 European cohorts: prospective analyses from the European Study of Cohorts for Air Pollution Effects (ESCAPE), The Lancet Oncology, 14(9), 813–822, doi:10.1016/S1470-2045(13)70279-1, 2013.

Randles, C. A., da Silva, A. M., Buchard, V., Colarco, P. R., Darmenov, A., Govindaraju, R., et al. (2017). The MERRA-2 Aerosol Reanalysis, 1980 Onward. Part I: System Description and Data Assimilation Evaluation. *Journal of Climate*, *30*(17), 6823–6850. http://doi.org/10.1175/JCLI-D-16-0609.1

Reeves, C. E., Formenti, P., Afif, C., Ancellet, G., Attié, J. L., Bechara, J., Borbon, A., Cairo, F., Coe, H., Crumeyrolle, S., Fierli, F., Flamant, C., Gomes, L., Hamburger, T., Jambert, C., Law, K. S., Mari, C., Jones, R. L., Matsuki, A., Mead, M. I., Methven, J., Mills, G. P., Minikin, A., Murphy, J. G., Nielsen, J. K., Oram, D. E., Parker, D. J., Richter, A., Schlager, H., Schwarzenboeck, A. and Thouret, V.: Chemical and aerosol characterisation of the troposphere over West Africa during the monsoon period as part of AMMA, Atmospheric Chemistry and Physics, 10(16), 7575–7601, doi:10.5194/acp-10-7575-2010, 2010.

Rienecker, M. M., *et al*. The GEOS-5 Data Assimilation System - Documentation of Versions 5.0.1, 5.1.0, and 5.2.0. *Technical Report Series on Global Modeling and Data Assimilation*, 27, NASA/TM–2008–104606, pp 118 (available at: http://gmao.gsfc.nasa.gov/pubs/docs/Rienecker369.pdf) (2008).

Schmidt, G. A., Kelley, M., Nazarenko, L., Ruedy, R., Russell, G. L., Aleinov, I., Bauer, M., Bauer, S. E., Bhat, M. K., Bleck, R., Canuto, V., Chen, Y.-H., Cheng, Y., Clune, T. L., Del Genio, A., de Fainchtein, R., Faluvegi, G., Hansen, J. E., Healy, R. J., Kiang, N. Y., Koch, D., Lacis, A. A., LeGrande, A. N., Lerner, J., Lo, K. K., Matthews, E. E., Menon, S., Miller, R. L., Oinas, V., Oloso, A. O., Perlwitz, J. P., Puma, M. J., Putman, W. M., Rind, D., Romanou, A., Sato, M., Shindell, D. T., Sun, S., Syed, R. A., Tausnev, N., Tsigaridis, K., Unger, N., Voulgarakis, A., Yao, M.-S. and Zhang, J.: Configuration and assessment of the GISS ModelE2

889 contributions to the CMIP5 archive, J. Adv. Model. Earth Syst., 6(1), n/a–n/a,
890 doi:10.1002/2013MS000265, 2014.

891 Schumann, U. and Huntrieser, H.: The global lightning-induced nitrogen oxides source,
892 Atmospheric Chemistry and Physics, 7(14), 3823–3907, doi:10.5194/acp-7-3823-2007, 2007.

893 Seltzer, K. M., Shindell, D. T., Faluvegi, G. and Murray, L. T.: Evaluating Modeled Impact
894 Metrics for Human Health, Agriculture Growth, and Near-Term Climate, J. Geophys. Res.
895 Atmos., 122(24), 13,506–13,524, doi:10.1002/2017JD026780, 2017.

896 Shah, A. S., Langrish, J. P., Nair, H., McAllister, D. A., Hunter, A. L., Donaldson, K., Newby, D.
897 E. and Mills, N. L.: Global association of air pollution and heart failure: a systematic review and
898 meta-analysis, The Lancet, 382(9897), 1039–1048, doi:10.1016/S0140-6736(13)60898-3, 2013.

899 Shindell, D. T., Pechony, O., Voulgarakis, A., Faluvegi, G., Nazarenko, L., Lamarque, J. F.,
900 Bowman, K., Milly, G., Kovari, B., Ruedy, R. and Schmidt, G. A.: Interactive ozone and methane
901 chemistry in GISS-E2 historical and future climate simulations, Atmospheric Chemistry and
902 Physics, 13(5), 2653–2689, doi:10.5194/acp-13-2653-2013, 2013.

903 Shindell, D., Faluvegi, G., Seltzer, K. and Shindell, C.: Quantified, localized health benefits of
904 accelerated carbon dioxide emissions reductions, Nature Climate change, 8(4), 1–7,
905 doi:10.1038/s41558-018-0108-y, 2018.

906 Silva, R. A., West, J. J., Lamarque, J.-F., Shindell, D. T., Collins, W. J., Faluvegi, G., Folberth,
907 G. A., Horowitz, L. W., Nagashima, T., Naik, V., Rumbold, S. T., Sudo, K., Takemura, T.,
908 Bergmann, D., Cameron-Smith, P., Doherty, R. M., Josse, B., MacKenzie, I. A., Stevenson, D. S.
909 and Zeng, G.: Future global mortality from changes in air pollution attributable to climate change,
910 Nature Climate change, 7(9), 647–651, doi:10.1038/nclimate3354, 2017.

911 Swap, R. J., Annegarn, H. J., Shuttles, J. T., Haywood, J., Heimlinger, M. C., Hely, C., Hobbs, P.
912 V., Holben, B. N., Ji, J., King, M. D., Landmann, T., Maenhaut, W., Otter, L., Park, B., Piketh, S.
913 J., Platnick, S., Privette, J., Roy, D., Thompson, A. M., Ward, D. and Yokeison, R.: The Southern
914 African Regional Science Initiative (SAFARI 2000): overview of the dry season field campaign,
915 South African Journal of Science, 1–6, 2002.

916 Thompson, A. M., Witte, J. C., Smit, H. G. J., Oltmans, S. J., Johnson, B. J., Kirchhoff, V. W. J.
917 H. and Schmidlin, F. J.: Southern Hemisphere Additional Ozonesondes (SHADOZ) 1998–2004
918 tropical ozone climatology: 3. Instrumentation, station-to-station variability, and evaluation with
919 simulated flight profiles, J. Geophys. Res., 112(D3), 23029–18, doi:10.1029/2005JD007042,
920 2007.

921 van Marle, M. J. E., Kloster, S., Magi, B. I., Marlon, J. R., Daniau, A.-L., Field, R. D., Arneth,
922 A., Forrest, M., Hantson, S., Kehrwald, N. M., Knorr, W., Lasslop, G., Li, F., Mangeon, S., Yue,
923 C., Kaiser, J. W. and van der werf, G. R.: Historic global biomass burning emissions for CMIP6
924 (BB4CMIP) based on merging satellite observations with proxies and fire models (1750–2015),
925 Geosci. Model Dev., 10(9), 3329–3357, doi:10.5194/gmd-10-3329-2017, 2017.

926 Wang, H., Abajobir, A. A., Abate, K. H., Abbafati, C., Abbas, K. M., Abd-Allah, F., Abera, S. F.,
927 Abraha, H. N., Abu-Raddad, L. J., Abu-Rmeileh, N. M. E., Adedeji, I. A., Adedoyin, R. A.,
928 Adetifa, I. M. O., Adetokunboh, O., Afshin, A., Aggarwal, R., Agrawal, A., Agrawal, S.,
929 Kiadaliri, A. A., Ahmed, M. B., Aichour, M. T. E., Aichour, A. N., Aichour, I., Aiyar, S.,

Akanda, A. S., Akinyemiju, T. F., Akseer, N., Lami, Al, F. H., Alabed, S., Alahdab, F., Al-Aly, Z., Alam, K., Alam, N., Alasfoor, D., Aldridge, R. W., Alene, K. A., Al-Eyadhy, A., Alhabib, S., Ali, R., Alizadeh-Navaei, R., Aljunid, S. M., Alkaabi, J. M., Alkerwi, A., Alla, F. O., Allam, S. D., Allebeck, P., Al-Raddadi, R., Alsharif, U., Altirkawi, K. A., Alvis-Guzman, N., Amare, A. T., Ameh, E. A., Amini, E., Ammar, W., Amoako, Y. A., Anber, N., Andrei, C. L., Androudi, S., Ansari, H., Ansha, M. G., Antonio, C. A. T., Anwari, P., v, J. Ã. R., Arora, M., Artaman, Al, Aryal, K. K., Asayesh, H., Asgedom, S. W., Asghar, R. J., Assadi, R., Assaye, A. M., Atey, T. M., Atre, S. R., Avila-Burgos, L., Avokpaho, E. F. G. A., Awasthi, A., Babalola, T. K., Bacha, U., Badawi, A., Balakrishnan, K., Balalla, S., Barac, A., Barber, R. M., Barboza, M. A., Barker-Collo, S. L., rnighausen, T. B., Barquera, S., Barregard, L., Barrero, L. H., Baune, B. T., Bazargan-Hejazi, S., Bedi, N., Beghi, E., jot, Y. B., Bekele, B. B., Bell, M. L., Bello, A. K., Bennett, D. A., Bennett, J. R., et al.: Global, regional, and national under-5 mortality, adult mortality, age-specific mortality, and life expectancy, 1970-2016: a systematic analysis for the Global Burden of Disease Study 2016, The Lancet, 390(10100), 1084–1150, doi:10.1016/S0140-6736(17)31833-0, 2017.

West, J. J., Cohen, A., Dentener, F., Brunekreef, B., Zhu, T., Armstrong, B., Bell, M. L., Brauer, M., Carmichael, G., Costa, D. L., Dockery, D. W., Kleeman, M., Krzyzanowski, M., Künzli, N., Liousse, C., Lung, S.-C. C., Martin, R. V., Pöschl, U., Pope, C. A., III, Roberts, J. M., Russell, A. G. and Wiedinmyer, C.: "What We Breathe Impacts Our Health: Improving Understanding of the Link between Air Pollution and Health," Environ. Sci. Technol., 50(10), 4895–4904, doi:10.1021/acs.est.5b03827, 2016.

WHO: 7 million premature deaths annually linked to air pollution, News release, World Health Organization, available at: http://www.who.int/mediacentre/news/releases/2014/air-pollution/en/, 2014.

WHO: Health risks of air pollution in Europe – HRAPIE: Recommendations of concentration-response functions for cost-benefit analysis of particulate matter, ozone and nitrogen dioxide, World Health Organization, available at: http://www.euro.who.int, 2013a.

WHO: Review of evidence on health aspects of air pollution (RE- VIHAAP), World Health Organization, WHO Technical Report, available at: http://www.euro.who.int , 2013b.

Winker, D. M., Vaughan, M. A., Omar, A., Hu, Y., Powell, K. A., Liu, Z., Hunt, W. H. and Young, S. A.: Overview of the CALIPSO Mission and CALIOP Data Processing Algorithms, J. Atmos. Oceanic Technol., 26(11), 2310–2323, doi:10.1175/2009JTECHA1281.1, 2009.

Wyzga, R. E. and Rohr, A. C.: Long-term particulate matter exposure: Attributing health effects to individual PM components, Journal of the Air & Waste Management Association, 65(5), 523–543, doi:10.1080/10962247.2015.1020396, 2015.

Yu, K., Jacob, D. J., Fisher, J. A., Kim, P. S., Marais, E. A., Miller, C. C., Travis, K. R., Zhu, L., Yantosca, R. M., Sulprizio, M. P., Cohen, R. C., Dibb, J. E., Fried, A., Mikoviny, T., Ryerson, T. B., Wennberg, P. O. and Wisthaler, A.: Sensitivity to grid resolution in the ability of a chemical transport model to simulate observed oxidant chemistry under high-isoprene conditions, Atmospheric Chemistry and Physics, 16(7), 4369–4378, doi:10.5194/acp-16-4369-2016, 2016.

Zuidema, P., Redemann, J., Haywood, J., Wood, R., Piketh, S., Hipondoka, M., Formenti, P., Redemann, J., Haywood, J., Piketh, S., Hipondoka, M. and Formenti, P.: Smoke and Clouds

above the Southeast Atlantic: Upcoming Field Campaigns Probe Absorbing Aerosol's Impact on Climate, https://doi.org/10.1175/BAMS-D-15-00082.1, 97(7), 1131–1135, doi:10.1175/BAMS-D-15-00082.1, 2016.